Theoretical Study on the Deoxyribose Radicals Formed by Hydrogen Abstraction

Karol Miaskiewicz and Roman Osman*

Contribution from the Department of Physiology and Biophysics, Mount Sinai School of Medicine of the City University of New York, New York 10029-6574

Received March 10, 1993. Revised Manuscript Received August 16, 1993®

Abstract: The structures of C_1, C_2, C_3, and C_4 centered deoxyribose radicals are optimized at the UHF/6-31G level. For each radical two puckered conformations are observed, which are significantly different from those of deoxyribose. In C_1 and C_2 radicals the pseudorotation angle, P, is shifted toward higher values compared to that of deoxyribose. In C_3 and C_4 radicals the shift of P is in the opposite direction. In addition, the puckering amplitude τ_m is significantly decreased in the radicals, indicating a flattening of the five-membered ring. The C_2 centered radical has the sp^2-type electronic structure, while C_1, C_3, and C_4 centered radicals are pyramidal. The enthalpies for H-atom abstraction from deoxyribose are calculated at the MP2/6-31G* level including ZPE and a scaling of correlation energy. The abstractions from C_1, C_3, and C_4 positions require similar energies, whereas the abstraction from the C_2 carbon of deoxyribose is less favorable by 3-4 kcal/mol. The susceptibility of different deoxyribose hydrogens for abstraction is estimated on the basis of their bond strength and their accessibility in nucleotides and in DNA.

Introduction

Deoxyribose radicals are key intermediates in producing strand breaks, which are the most severe form of lesion in radiation damage to DNA. These radicals are formed in the reaction between products of water radiolysis (e.g., •OH radicals) and the sugar moiety of DNA. The extent of •OH attack on sugar is too low to account for the observed yield of strand breaks. For example, in poly(U), only 7% of OH radicals attack the sugar moiety and the rest add to the uracil base.[1] Since the efficiency of an OH radical in producing strand breaks is much greater (≈40%) than the 7% accounted for by H-abstraction from the sugar, a process must exist in which sugar radicals are formed in a reaction between the base radical (major product of •OH attack) and the sugar moiety.[1] Strong evidence for sugar radicals formation by base radicals comes from ESR and laser pulse experiments.[2-4] In these experiments the laser pulse produces only base radical cations because the sugars are not directly affected by laser light. However, high yields of strand breaks are observed, demonstrating the involvement of base radicals in strand break formation through the intramolecular process of H-abstraction from the sugar.

While the base radicals are formed in addition reactions, sugar radicals are formed exclusively in hydrogen abstraction processes. From product studies on simple carbohydrates such as D-glucose, it has been concluded[5,6] that •OH attack at various C-H sugar bonds is rather random. However, a small preference for the abstraction from the carbon adjacent to the alicyclic oxygen has been observed for the furanose ring.[7,8] Radiation-induced formation of radicals in different nucleosides and nucleotides together with poly(U) have been extensively studied by ESR and spin-trapping methods in series of works by Kuwabara et al.[9-16] In all the molecules studied, radicals localized on C_1', C_4', and C_5' atoms have been detected. No C_2' or C_3' centered radicals have been observed. On the other hand, the ESR spectra of H•-induced radicals of purine nucleosides (-tides) formed in frozen acidic glasses were interpreted in terms of C_1', C_2', C_3', and C_5' centered radicals for ribosides and C_1', C_2', and C_5' centered radicals for deoxyribosides. In the single crystals of 2'-deoxyguanosine 5'-monophosphate irradiated at high doses of X-radiation, all the carbon centered (C_1', C_2', C_3', C_4', and C_5') deoxyribose radicals have been observed recently by ENDOR spectroscopy.[17] Stable products observed in γ-irradiated aqueous solutions of calf thymus DNA in the absence of oxygen have been correlated with C_1', C_4', and C_5' as well as C_2' centered sugar radicals as the precursors for those products.[18]

It is widely accepted that, in the absence of oxygen, strand breaks in irradiated DNA are due to sugar-phosphate bond cleavage at the β-position to the C_4' radical of deoxyribose. In RNA, on the other hand, reactions similar to those for C_4' can be also written for the C_2' radical. Thus, in poly(U), the β-cleavage can originate either from the C_4' radical formed through H-abstraction by the OH• radical or from the C_2' radical, which is postulated to be formed through the intramolecular H-abstraction by the base radical.[2] These two mechanisms are possible because the hydroxy group on C_2' of the ribose, which does not exist in deoxyribose, can enhance strand break formation through β-cleavage. The question whether a C_2' radical of deoxyribose can lead to a strand break in DNA remains open. Another

* Abstract published in *Advance ACS Abstracts,* December 1, 1993.

(1) Deeble, D. J.; Schulz, D.; von Sonntag, C. *Int. J. Radiat. Biol.* **1986**, *49*, 915-926.
(2) Hildebrand, K.; Schulte-Frohlinde, D. *Int. J. Radiat. Biol.* **1989**, *55*, 725-738.
(3) Wala, M.; Bothe, E.; Görner, H.; Schulte-Frohlinde, D. *J. Photochem. Photobiol., A* **1990**, *53*, 87-108.
(4) Bothe, E.; Görner, H.; Opitz, J.; Schulte-Frohlinde, D.; Siddiqi, A.; Wala, M. *Photochem. Photobiol.* **1990**, *52*, 949-959.
(5) Schuchmann, M. N.; von Sonntag, C. *J. Chem. Soc., Perkin Trans. 2* **1977**, 1958-1963.
(6) Madden, K. P.; Fessenden, R. W. *J. Am. Chem. Soc.* **1982**, *104*, 2578-2581.
(7) Gilbert, B. C.; King, D. M.; Thomas, C. B. *J. Chem. Soc., Perkin Trans. 2* **1983**, 675-683.
(8) Fitchett, M.; Gilbert, B. C. *J. Chem. Soc., Perkin Trans. 2* **1988**, 673-689.
(9) Kuwabara, M.; Zhi-Yi, Z.; Yoshii, G. *Int. J. Radiat. Biol.* **1982**, *41*, 241-259.
(10) Inanami, O.; Kuwabara, M.; Endoh, D.; Sato, F. *Radiat. Res.* **1986**, *108*, 1-11.
(11) Inanami, O.; Kuwabara, M.; Sato, F. *Radiat. Res.* **1987**, *112*, 36-44.
(12) Kuwabara, M.; Hiraoka, W. *Free Radical Res. Commun.* **1989**, *6*, 97-98.
(13) Kuwabara, M.; Hiraoka, W.; Sato, F. *Biochemistry* **1989**, *28*, 9625-9632.
(14) Hiraoka, W.; Kuwabara, M.; Sato, F. *Int. J. Radiat. Biol.* **1989**, *55*, 51-58.
(15) Hiraoka, W.; Kuwabara, M.; Sato, F.; Matsuda, A.; Ueda, T. *Nucleic Acids Res.* **1990**, *18*, 1217-1223.
(16) Hiraoka, W.; Kuwabara, M.; Sato, F. *Int. J. Radiat. Biol.* **1991**, *59*.
(17) Hole, E. O.; Nelson, W. H.; Sagstuen, E.; Close, D. M. *Radiat. Res.* **1992**, *129*, 119-138.
(18) Schulte-Frohlinde, D.; von Sonntag, C. In *Ionizing Radiation Damage to DNA: Molecular Aspects*; Wiley-Liss, Inc.: New York, 1990; pp 31-42.

0002-7863/94/1516-0232$04.50/0 © 1994 American Chemical Society

Scheme 1

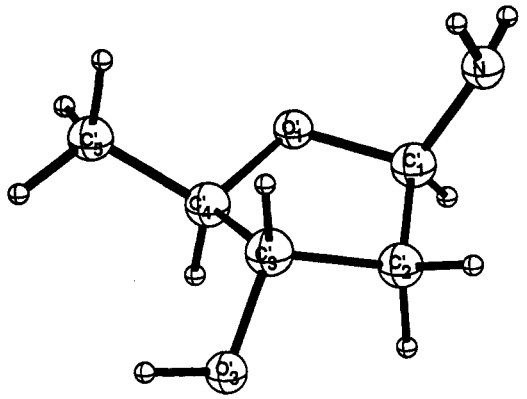

important property that may be related to strand break formation is the conformation of the sugar radical. This has been suggested as the possible cause for the selective cleavage at the 3′ side of dApdA and other model compounds.[19]

Thus, understanding the properties of primary radicals generated by H-abstraction from deoxyribose is essential in investigating the pathways of radiation damage to DNA. In this study we present results of extended *ab initio* calculations of structures and properties of radicals formed by H-abstraction from different positions of the deoxyribose sugar ring.

Methods

All the quantum chemical calculations were performed with GAUSSIAN88[20] and GAUSSIAN90[21] systems of programs for *ab initio* calculations. Deoxyribose has been modeled by (*R*)-2-amino-(*S*)-4-hydroxy-(*S*)-5-methyltetrahydrofuran (2,5-dideoxy-β-D-*erythro*-pentafuranosylamine) shown in Scheme 1. Since only the abstraction of hydrogens in the ring of deoxyribose was investigated in this work, the 5-OH group was not included in the model. The base was modeled by an amino group. It is assumed that the absence of the 5-OH group and the simple model of the base will have small effects on the structure or the strength of the C–H bonds in the ring. The closest atom to the 5-OH group is H_4, which is in a β-position with respect to that group, and the effect of the polar group is largely attenuated at this distance. Also, the polarity of the base attached through a nitrogen atom to the sugar is modeled by the NH_2 group; the rest of the base has probably a small effect on the structure of deoxyribose and the C–H bond strength.

The structure of this model of deoxyribose and the radicals formed by H-abstraction from C_1, C_2, C_3, and C_4 positions were fully optimized at the HF/6-31G level. The initial geometries used for the optimization of the radicals were taken from the structures of deoxyribose, and all internal coordinates were optimized. Frequency analysis of the optimized structure confirmed that they are local minima on the potential energy surface. The expectation value of S^2 in open shell molecules did not exceed the value of 0.764 before anihilation of the first contaminant. The correlated energy was calculated at the MP2/6-31G* level for each of the optimized structures. The zero point energy (ZPE) and the enthalpy correction to room temperature ($H_{(298°)} - H_{(0°)}$) were evaluated as suggested by Pople et al.[22] on the basis of 6-31G frequencies obtained for the HF/6-31G optimized structures. The correlation energies were scaled with a scaling factor $f_2 = 0.66$ using the method described by Gordon and Truhlar.[23]

The conformations of the sugar ring are discussed in terms of the pseudorotation phase angle which can be calculated according to the following formula:[24]

$$\tan P = \frac{(\nu_4 + \nu_1) - (\nu_3 + \nu_0)}{2\nu_2(\sin 36° + \sin 72°)}$$

where ν_j are the ring dihedral angles defined as follows: $\nu_0 = C_4O_1C_1C_2$; $\nu_1 = O_1C_1C_2C_3$; $\nu_2 = C_1C_2C_3C_4$; $\nu_3 = C_2C_3C_4O_1$; $\nu_4 = C_3C_4O_1C_1$. The puckering amplitude, τ_m, is defined as

$$\tau_m^2 = {}^2/_5 \sum_{j=0}^{4} \nu_j^2$$

Results and Discussion

Structure of the Sugar Ring. Deoxyribose. According to X-ray crystallographic studies, the sugar ring in nucleic acids can adopt one of the two principal puckering states; ^3E (C_3'-*endo*) and ^2E (C_2'-*endo*) with minor variants. These two forms correlate with two distinctly different DNA families: the C_3'-*endo* puckered state is observed in A-DNA and the C_2'-*endo* in B-DNA structures.

Optimizations of the structure of the model of deoxyribose used in this work produce two energy minima that correspond to the ^2E and ^3E puckering states. The structural parameters for these conformers are shown in Table 1 together with experimental values obtained from a compilation of X-ray crystallographic structures of nucleotides and nucleosides.[25,26] Clearly the structural parameters of the optimized structures are in excellent agreement with the compiled values. The amplitude of puckering, τ_m, is in the range of values observed in the crystal data but slightly lower than the mean value derived from the compilation. The ring torsional angles in the calculated structures are close to the mean experimental values published by Arnott,[25] indicating that the calculated puckering in deoxyribose is very similar to that observed in crystallographic structures of nucleosides and nucleotides. The sums of the cyclic angles in the calculated structures agree very well with those observed experimentally. The agreement for individual ring angles is less good, but the difference does not exceed 3°. In the experimental structures the ring internal angles always follow the trend C–O–C > C–C–O > C–C–C. In the calculated structures the C–O–C angle is the largest, but there is no meaningful difference between the C–C–O and C–C–C angles. According to the work of Westhof and Sundaralingam,[27] at a fixed τ_m, the variations with *P* of endocyclic C_1 and C_4 angles are higher than those of C_2 and C_3 angles. This can also be observed in the optimized structures; the difference between $C_2C_1O_1$ and $O_1C_4C_3$ in ^2E and ^3E puckered states is clearly larger than for the remaining ring angles.

The calculated bond lengths for deoxyribose agree well with experimental values, except the O_1C_1 bond, which is clearly longer in the calculated structures. It is possible that the presence of a highly polar amino group at C_1 in our model is responsible for this effect. Both O_1 and N atoms are highly negative, and the electrostatic interaction might contribute to the lengthening of the C_1O_1 bond.

Thus, the calculated geometries of the present model of deoxyribose conformers agree very well with crystallographic structures of nucleosides and nucleotides[25,26] in spite of the fact that the calculations simulate gas-phase structures of a model compound that includes a polar amino group at C_1 position, which

(19) Ito, T.; Saito, M.; Kobayashi, K. *Int. J. Radiat. Biol.* **1992**, *62*, 129–136.

(20) Frish, M. J.; Head-Gordon, M.; Schlegel, H. B.; Raghavachari, K.; Binkley, J. S.; Gonzalez, C.; Defrees, D. J.; Fox, D. J.; Whiteside, R. A.; Seeger, R.; Melius, C. F.; Baker, J.; Martin, R.; Kahn, L. R.; Stewart, J. J. P.; Fluder, E. M.; Topiol, S.; Pople, J. A. *GAUSSIAN 88*; Gaussian, Inc .: Pittsburgh, PA, 1988.

(21) Frisch, M. J.; Head-Gordon, M.; Trucks, G. W.; Foresman, J. B.; Schlegel, H. B.; Raghavachari, K.; Robb, M.; Binkley, J. S.; Gonzalez, C.; Defrees, D. J.; Fox, D. J.; Whiteside, R. A.; Seeger, R. A. R.; Melius, C. F.; Baker, J.; Martin, R. L.; Kahn, L. R.; Stewart, J. J. P.; Topiol, S.; Pople, J. A. *GAUSSIAN90*; Gaussian, Inc.: Pittsburgh, PA, 1990.

(22) Pople, J. A.; Schlegel, H. B.; Krishnan, R.; Defrees, D. J.; Binkley, J. S.; Frish, M. J.; Whiteside, R. A.; Hout, R. J.; Hehre, W. J. *Int. J. Quantum Chem., Symp.* **1981**, *S15*, 269.

(23) Gordon, M. S.; Truhlar, D. G. *J. Am. Chem. Soc.* **1986**, *108*, 5412–5419.

(24) Altona, C.; Sundaralingam, M. *J. Am. Chem. Soc.* **1972**, *94*, 8205–8212.

(25) Arnott, S.; Hukins, D. W. L. *Biochem. J.* **1972**, *130*, 453–465.

(26) Saenger, W. *Principles of Nucleic Acid Structure*; Springer-Verlag: New York, 1984.

(27) Westhof, E.; Sundaralingam, M. *J. Am. Chem. Soc.* **1980**, *102*, 1493–1500.

Table 1. Structural Parameters of the Conformers of Deoxyribose and Its Radicals

	deoxyribose[a]		C_1 radical		C_2 radical		C_3 radical		C_4 radical	
	^2E	^3E	^2E	$_4E$	^2_3T	$_4E$	^0E	$_2E$	$_1E$	$_2E$
Puckering Parameters (deg)										
phase angle, *P*	153.9 (165)	18.3 (2–20)	164.1	55.2	180.7	64.5	84.4	−21.0	136.0	−14.4
τ_m	36.9 (35–41)	35.6 (35–41)	29.9	34.4	19.1	29.9	31.0	29.0	31.9	34.1
Endocyclic Torsional Angles (deg)										
ν_0	−26.1 (−23.5)	−0.3 (3.2)	−17.2	−21.3	−5.3	−22.0	−31.2	19.0	−28.5	18.8
ν_1	35.9 (36.9)	−21.1 (−25.6)	28.2	−0.1	15.5	4.4	19.5	−27.0	31.1	−31.6
ν_2	−33.1 (−35.7)	33.7 (36.9)	28.2	19.5	−19.2	12.8	−3.0	27.1	−22.7	32.4
ν_3	17.7 (22.9)	−33.6 (−35.9)	18.8	−31.8	15.1	−25.2	−14.8	−16.2	6.3	−22.4
ν_4	5.4 (0.2)	21.5 (20.8)	−1.4	33.3	−6.3	30.5	28.7	−2.2	14.3	2.5
Exocyclic Torsional Angles (deg)										
$N_1C_1C_2C_3$	157.2	100.8	167.4	140.1	138.4	126.1	141.5	95.8	147.1	83.5
$H_1C_1C_2C_3$	−79.2	−136.1			−99.0	−110.7	−95.7	−141.1	−83.2	−146.7
$H_{2A}C_2C_3C_4$	83.8	155.6	90.4	141.2	172.4	−173.8	115.4	147.7	92.7	154.1
$H_{2B}C_2C_3C_4$	−155.0	−84.0	−149.4	−99.6			−123.3	−90.4	−145.4	−84.6
$O_3C_3C_4O_1$	−99.7	−158.5	−99.5	−157.6	−103.4	−149.8	−157.4	−158.3	−112.9	−143.3
$H_{O3}O_3C_3C_4$	−179.2	65.9	174.8	67.3	176.2	71.3	−171.2	−174.5	−170.3	−162.4
$H_3C_3C_4O_1$	140.4	84.9	141.0	86.4	137.4	94.3			127.0	95.7
$C_5C_4O_1C_1$	128.3	145.5	121.3	156.8	116.5	154.6	151.9	121.6	168.6	152.7
$H_4C_4O_1C_1$	−110.6	−94.0	−117.6	−82.3	−122.6	−84.8	−87.4	−118.3		
Endocyclic Angles (deg)										
$C_1O_1C_4$	111.7 (109.5)	112.6 (110.5)	111.5	109.3	113.6	111.7	110.8	113.1	110.0	110.7
$C_2C_1O_1$	102.5 (105.8)	104.2 (106.9)	107.3	108.4	103.1	102.6	104.1	104.2	103.4	104.3
$C_3C_2C_1$	103.3 (101.8)	104.3 (102.3)	103.1	103.9	110.6	110.8	103.5	102.2	104.0	102.6
$C_4C_3C_2$	103.9 (102.1)	103.0 (102.8)	104.3	104.1	103.5	102.7	110.0	109.3	103.2	102.3
$O_1C_4C_3$	105.1 (106.0)	103.6 (104.8)	105.2	103.0	105.8	104.3	102.6	103.2	109.6	108.6
sum of endocyclic angles	526.5 (525.2)	527.7 (527.3)	531.4	528.7	536.6	532.1	531.0	532.0	530.2	528.5
Bond Lengths (Å)										
C_1C_2	1.526 (1.517)	1.536 (1.526)	1.501	1.511	1.499	1.503	1.541	1.535	1.531	1.529
C_2C_3	1.525 (1.523)	1.531 (1.523)	1.531	1.539	1.493	1.498	1.507	1.504	1.536	1.535
C_3C_4	1.538 (1.521)	1.531 (1.526)	1.539	1.537	1.538	1.541	1.506	1.503	1.502	1.500
C_4O_1	1.445 (1.447)	1.440 (1.452)	1.449	1.442	1.448	1.441	1.441	1.446	1.395	1.402
O_1C_1	1.456 (1.420)	1.463 (1.414)	1.410	1.416	1.454	1.460	1.457	1.459	1.441	1.440

[a] In parentheses are the experimental values for deoxyribose, as obtained from a compilation of X-ray structures of nucleosides and nucleotides.[24,25]

is not present in nucleosides and nucleotides. Evidently, many geometrical characteristics of deoxyribose are intrinsic features, which are only moderately affected by the molecular or the physical environment.

In contrast the puckering of the five-member ring is much more sensitive to the nature of substituents. Recently the structures of 2-deoxy-β-D-*glycero*-tetrofuranose have been calculated with the 3-21G and the 6-31G* basis sets.[28,29] The difference between this molecule and the model of deoxyribose presented in this work is that the amino group is replaced by OH and the CH_3 attached to C_4 is missing. Two energetic minima have also been found,[28] but at significantly different pseudorotation phase angles than in the model compound presented here. The S-type conformer was found to be a ^4E (C_4-*endo*) and the N-type conformer a $_2E$ (C_2-*exo*). Thus, the minima on the pseudorotation path are significantly shifted in comparison to our results. Because similar results were obtained with the 6-31G* basis set,[29] it is reasonable to suggest that substituent effects are of major importance in determining the puckering of the sugar ring.

Total and relative energies of the optimized structures are shown in Table 2. At each level of calculations the ^2E structure is more stable. At MP2/6-31G* level the energy difference corrected for ZPE is 1.63 kcal/mol. This value has not been measured directly by experiment. However, the interconversion between deoxyribose puckered states has been observed in the solid-state ^2H NMR of methylated deoxythymidine.[30] The major conformer has been assigned as C_3'-*exo*. This conformer is structurally similar to C_2'-*endo*. Its pseudorotation phase angle is 196° as compared to 154° for C_2'-*endo*. The estimated population of this conformer at 25 °C is 95%. This translates to an energetic difference of 1.77 kcal/mol between the puckered conformations, which agrees very well with the calculated value for the present deoxyribose model. The *ab initio* calculations of 2-deoxy-β-D-*glycero*-tetrofuranose[28] also show a preference for the S-type structure by about 1 kcal/mol (HF/6-31G*), which is similar to the value observed in our calculations (1.2 kcal/mol at the HF/6-31G*).

Hydration can be expected to affect the relative stabilization of the conformers. However, on the basis of dipole moments values, the ^2E structure (μ = 2.70 D) should be more stabilized than the ^3E (μ = 0.97 D), and thus hydration may slightly increase the preference for the ^2E structure.

Deoxyribose Radicals. The structural parameters of the four carbon centered radicals are shown in Table 1 and their energies in Table 2. The formation of the radical center causes significant disturbance of the sugar geometry (Table 1). However, it should be noticed that structural changes are very local, i.e., they are limited to the radical center and the geometrical parameters of the rest of the ring are only slightly disturbed.

Two conformations have also been found for the sugar radicals, but their structures differ from those observed for deoxyribose. The major structural difference is observed in the ring pseudorotation angles (Table 1, Figure 1). In C_1 and C_2 radicals the pseudorotation phase angle, *P*, is shifted to higher values than in deoxyribose. In C_3 and C_4 radicals *P* is shifted in the opposite direction. In the C_3 radical, the pseudorotation phase angle of both conformers is in the range of the northern hemisphere. However, since the O_1'-*endo* is very close to 90°, i.e., an *E*-conformation, for consistency of presentation, it has been arbitrary assigned as an S-type. Changes in the puckered state of deoxyribose are related to the decreased amplitude of puckering

(28) Garrett, E. C.; Serianni, A. S. *Carbohydr. Res.* **1990**, *206*, 183–191.
(29) Garrett, E. C.; Serianni, A. S. In *Computer Modeling of Carbohydrate Molecules*; French, A., Brady, J., Eds.; American Chemical Society: Washington, DC, 1990; Vol. 430, pp 91–119.
(30) Hiyama, Y.; Siddharta, R.; Cohen, J. S.; Torchia, D. A. *J. Am. Chem. Soc.* **1989**, *111*, 8609–8613.

Table 2. Energies and Dipole Moments of Conformers of Deoxyribose and Radicals of Deoxyribose

	energy (hartrees) (ZPE in kcal/mol)		energy difference, (N-type) – (S-type) (kcal/mol)
	S-type puckering	N-type puckering	
	Deoxyribose		
	^{2}E (C_2-endo)	^{3}E (C_3-endo)	
HF/6-31G	–399.731 749	–399.729 107	1.66
HF/6-31G*	–399.896 431	–399.894 525	1.20
MP2/6-31G*	–401.064 092	–401.061 224	1.80
ZPE	100.10	99.93	–0.17
μ (D)	2.70	0.97	
	C_1 Radical		
	^{2}E (C_2-endo)	$_4$E (C_4-exo)	
HF/6-31G	–399.108 318	–399.108 490	–0.11
HF/6-31G*	–399.271 000	–399.271 434	–0.27
MP2/6-31G*	–400.413 172	–400.413 102	0.04
ZPE	91.62	91.61	–0.01
μ (D)	3.27	0.92	
	C_2 Radical		
	$^2_3$T (twisted)	$_4$E (C_4-exo)	
HF/6-31G	–399.103 194	–399.104 563	–0.86
HF/6-31G*	–399.265 049	–399.268 129	–1.93
MP2/6-31G*	–400.403 688	–400.406 582	–1.81
ZPE	91.33	91.35	0.02
μ (D)	2.81	1.16	
	C_3 Radical		
	^{0}E (O_1-endo)	$_2$E (C_2-exo)	
HF/6-31G	–399.108 697	–399.108 470	0.14
HF/6-31G*	–399.273 292	–399.271 984	0.82
MP2/6-31G*	–400.413 366	–400.412 883	0.30
ZPE	91.90	91.95	0.05
μ (D)	1.99	2.34	
	C_4 Radical		
	$_1$E (C_1-exo)	$_2$E (C_2-exo)	
HF/6-31G	–399.100 501	–399.104 756	–2.67
HF/6-31G*	–399.266 421	–399.270 382	–2.49
MP2/6-31G*	–400.407 119	–400.411 143	–2.53
ZPE	91.05	91.58	0.53
μ (D)	2.90	2.20	

(Table 1), which causes a distinctive flattening of the sugar ring. The flattening is largest in the C_2 radical (for the $^2_3$T structure, τ_m is only 19.1°), and the smallest for C_4 (τ_m = 34.1° for the $_2$E conformer) and C_1 (τ_m = 34.4° for the $_4$E structure) radicals. In the $^2_3$T structure of the C_2 radical the sum of endocyclic angles is 536.6°, which is very close to 540°, the value expected for an ideal planar five-membered ring. It should be noted that τ_m values for sugar radicals show essential variations with the puckering angle. The pseudorotation path is often considered to occur with a constant amplitude, but the observed variations in τ_m clearly indicate that this concept is only an approximation of the dynamics of the furanose ring.

Another way of representing the flatening of the deoxyribose ring is through the improper dihedral angles at the carbon on which the radical is centered shown in Table 3. The C_2 radical adopts an almost planar configuration with improper dihedral angles around 170°. In this respect, it represents the largest flatening because the structure at the other radical centers is more pyramidal with improper dihedral angles in the range 135–149°. The more pyramidal nature of these radicals can be related to their proximity to the oxygen atom. C_1 and C_4 radicals are positioned α to O_1, and C_3, α to the exocyclic hydroxyl group, whereas C_2 has no oxygen in an α position. The high charge density on the oxygen prevents the formation of a planar radical because of the repulsion it exerts on the unpaired electron. Retaining a pyramidal geometry will minimize such interactions. The radical centered on C_2 feels no such repulsion, and therefore it becomes much more flat than all the other radicals.

The tendency of ring flattening induced by the formation of the radical can provide an explanation for the shift of the sugar

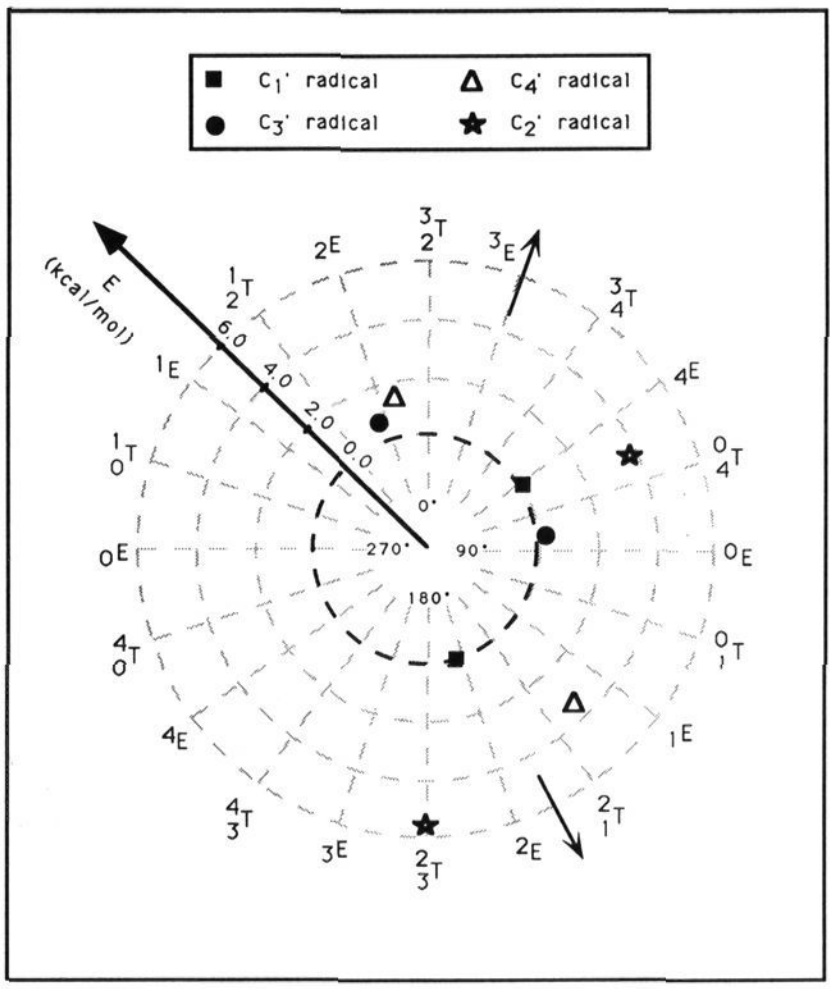

Figure 1. Positions of deoxyribose radicals on a pseudorotation wheel. The radial coordinate is the energy of the radical relative to that of the C_1 radical. The positions of deoxyribose puckered conformers are included for comparison (arrows).

Table 3. Improper Dihedral Angles at the Carbon on Which the Radical is Centered

	improper dihedral angle[a] (deg)	X1	X2	X3
C_1 radical		O_1	N	C_2
^{2}E	135.4			
$_4$E	137.1			
C_2 radical		C_1	H_2	C_3
$^2_3$T	167.1			
$_4$E	172.6			
C_3 radical		C_4	O_3	C_2
^{0}E	137.5			
$_2$E	136.7			
C_4 radical		C_3	C_5	O_1
$_1$E	148.9			
$_2$E	144.3			

[a] The improper dihedral angle is defined as the dihedral angle between planes X1–C–X2 and X2–C–X3. The respective angles in deoxyribose are in the range 114–117°.

ring puckering in deoxyribose radicals. Because of the flattening, formation of a radical center causes a change in the torsional angles, in which the radical center is involved, in the direction of bringing them closer to zero. This is illustrated in Figure 2, which shows that the changes in the torsional angles around bonds flanking the radical center in the direction closer to zero cause a change in the pseudorotation angles which correspond to the observed changes. Two exceptions should be noted: the change in ν_0 in the C_1 radical in the $_4$E form and the change in ν_4 in the C_4 radical in the $_1$E form. In both cases the original angles in deoxyribose are close to zero, indicating a conformation in which the radical that is formed is eclipsed with the lone pair of the oxygen. Thus, the flattening of the radical center taken together with the repulsion between the unpaired electron and the lone pair on the adjacent oxygen must result in the observed movement and associated change in the torsional angles. These interactions are illustrated on Figure 3 for the $_1$E conformation of the C_4 radical. On the one hand, the change of the puckering phase angle from 154° in deoxyribose to 136° in the C_4 radical brings the ν_3 dihedral angle ($C_2C_3C_4O_1$) closer to zero (flattening of

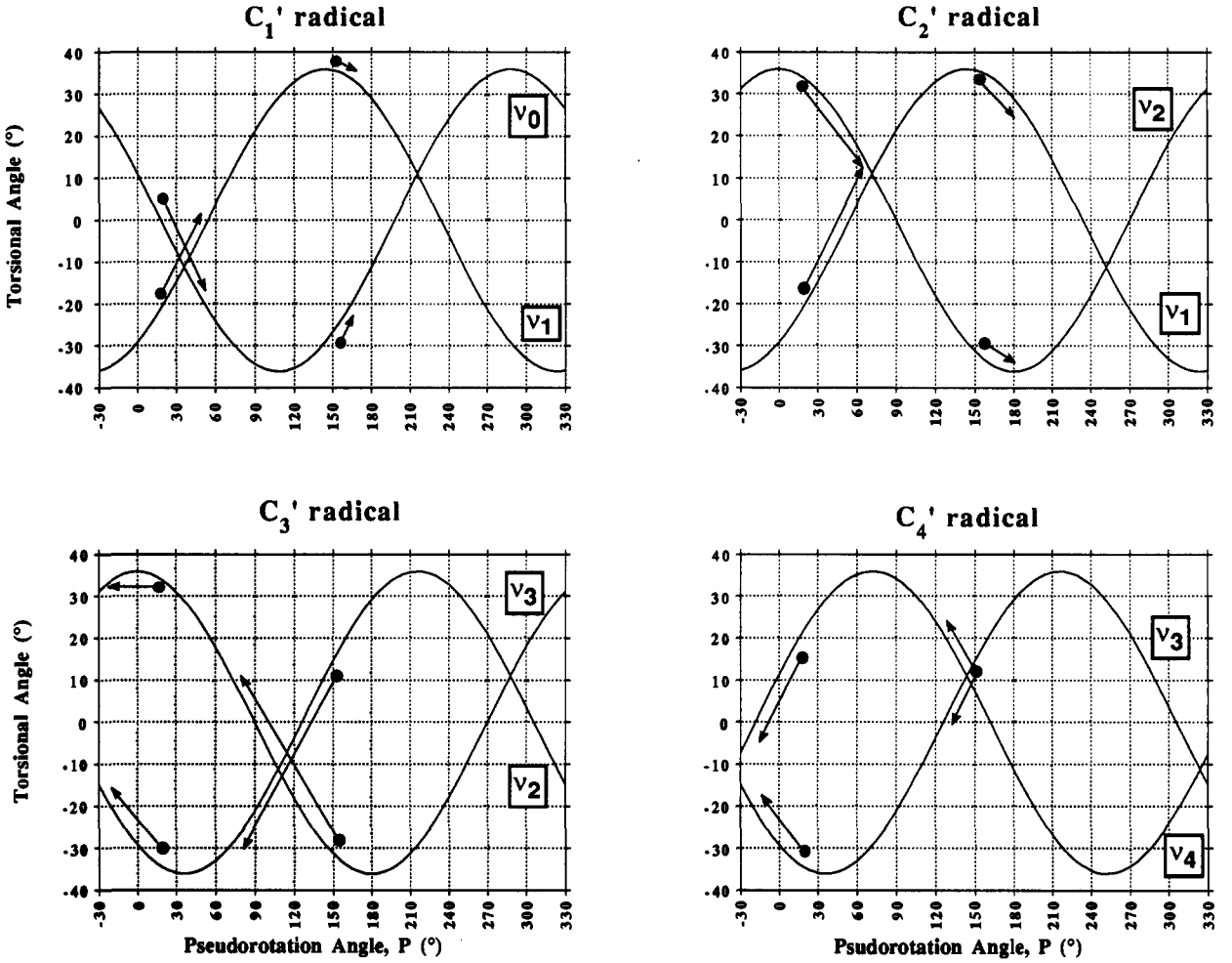

Figure 2. Plots of torsional angles involving the radical center as a function of the pseudorotation phase angle. The arrows show the observed shifts of the deoxyribose pseudorotation phase angles upon the formation of radicals.

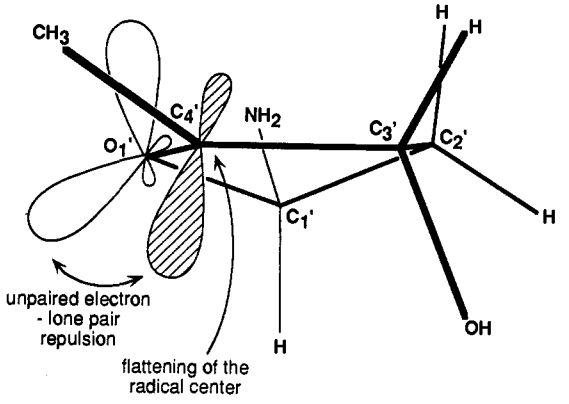

Figure 3. Example of the electronic interactions that influence the puckering of deoxyribose radicals illustrated on the $_1$E structure of the C_4 radical.

radical center), and on the other hand, it increases ν_4 ($C_3C_4O_1C_1$), which effectively decreases the repulsion between the unpaired electron and the O_1 lone pair. The change in puckering of the C_4 radical in the opposite direction could help bring ν_4 to zero, but at the same time it would increase the electronic repulsion with the oxygen lone pair.

The relative energies of the radicals centered on the same carbon are different from those of deoxyribose. In the radicals the energetic preference for the S-type conformer is no longer observed (Table 2, Figure 1). In C_1 and C_3 radicals the energy of the conformers is almost the same. In C_2 and especially in C_4 radicals, the N-type structure has significantly lower energy than the S-type. Because the calculated energies refer to the molecules in the gas phase, it is expected that solvation energy may significantly affect the relative stabilization of conformers. The calculated dipole moment values (Table 2) show that hydration should preferentially stabilize the S-type conformer because the dipole moments of S-type structures are somewhat higher than the dipole moments of the N-type conformers. In the C_3 radical, the dipole moments for both conformers are similar. Thus there should be only a small effect of hydration of their relative stabilities.

Electronic Properties of Deoxyribose Radicals. The special electronic properties of deoxyribose radicals are related to the density distribution of the unpaired electron. The spin density in the radicals of deoxyribose is highly localized on the carbon from which the hydrogen was abstracted: 87% for the C_1 radicals, 93% for the C_2 radical, 89% for the C_3 radical, and 88% for the C_4 radical as calculated from ROHF wave functions. In C_1, C_3, and C_4 radicals a significant amount of spin density (5–6%) is observed on the oxygen atom adjacent to the radical center, i.e. on O_1 in C_1 and C_4 radicals and on O_3 in the C_3 radical. The interaction with these oxygens is responsible for the pyramidal structure of the radicals, as discussed above. The C_2 radical lacks this interaction and therefore has the nearly planar structure. Consistent with the near planar geometry of the C_2 radical, the spin is localized mostly in p-type orbitals with a very small contribution from the s atomic orbitals (Table 4). The contribution from the s atomic orbitals is much higher for C_1, C_3, and C_4 radicals, showing that the unpaired electron occupies a hybridized orbital. This is consistent with the higher degree of pyramidality of these atoms. The contribution of the s atomic orbitals is largest in the C_1 radical, possibly because of the presence

Table 4. Total Spin Density in Deoxyribose Radicals Summed over s and p Atomic Orbitals

	total spin density over	
	s orbitals	p orbitals
	C_1 radical	
^2E	0.34	0.66
$_4E$	0.33	0.67
	C_2 radical	
^2_3T	0.10	0.90
$_4E$	0.13	0.87
	C_3 radial	
^0E	0.28	0.72
$_2E$	0.30	0.70
	C_4 radical	
$_1E$	0.28	0.72
$_2E$	0.26	0.74

Table 5. Isotropic Hyperfine Coupling Constants (MHz) Calculated from the Fermi Contact Analysis of the UHF Wave Functions

	C_1 radical ^2E	C_2 radical $_4E$	C_3 radical ^0E	C_4 radical $_2E$
carbon (^{13}C)[a]	463.1	308.9	405.9	393.9
H_1		94.2		
H_{2A}	41.7	−146.0	52.2	
H_{2B}	97.7		95.7	
H_3		106.6		85.7
H_4			74.7	
H_5				63.2[b]

[a] Coupling constants for ^{13}C on which the radical is centered. [b] Averaged value for the protons of the 5-methyl group.

of two atoms (O_1 and N) with high electron density attached to this carbon. It is interesting to note that the analysis of EPR and ENDOR spectra of deoxyribose radicals in irradiated single crystals of deoxygunosine[17] has led to very similar conclusions: sp^2 configuration at C_2' in the C_2' centered radical, but not complete rehybridization at C_3' carbon in the C_3' centered radical. Our calculations indicate that C_1 and C_4 radicals are electronically similar to C_3 with a partial pyramidalization of radical centers.

Table 5 displays the isotropic hyperfine coupling constants calculated form the Fermi contact analysis of the UHF wave function. Only the electron density of s-type orbitals contributes to the Fermi contact interaction, and therefore the hyperfine coupling for the radical centered carbon nucleus is much smaller for the C_2 radical than for other sugar radicals. Furthermore, the hyperfine coupling with a nitrogen nucleus is almost three times larger in the C_2 radical than in the C_1 radical, despite the fact that in the C_1 radical the unpaired electron is centered on the carbon adjacent to the nitrogen. However, the amino group in our model is probably not a very good representation of the base nitrogen, and the observed electronic properties of this amino nitrogen may not be a good model of the situation in nucleosides or nucleotides.

Recently, all carbon centered deoxyribose radicals have been observed with ENDOR spectroscopy in X-irradiated single crystals of 2′-deoxyguanosine 5′-monophosphate.[17] Both isotropic and anisotropic hydrogen hyperfine couplings were extracted from the ENDOR spectra. The calculated values presented in Table 5 can be compared directly with the isotropic hyperfine couplings measured by Hole et al.[17] For the C_1' centered radical two β-couplings were observed with isotropic values of 78.4 and 45 MHz. The calculated values for H_2 protons in the C_1 radical are 97.7 and 41.7 MHz, respectively. For the C_2' centered radical the α-coupling with an isotropic value of −64.8 MHz and the β-coupling with a value of 90.9 MHz were measured. The values calculated from the Fermi contact interaction are −146.0 and 94.2 MHz for H_{2A} and H_1, respectively. The coupling with H_3' was not observed in the ENDOR spectrum. Our calculations indicate that this coupling should be very similar in value to that from the H_1 proton. In the C_3' radical three β-couplings from two H_2' and the H_4' protons with values of 46.8 MHz (H_{2B}'), 77.1 MHz (H_4'), and 106.9 MHz (H_{2A}') were observed. The respective calculated values are 52.2, 74.7, and 95.7 MHz. The observed spectrum of the C_4' radical was consistent with an open furanose ring structure due to breakage of the C_4'–O_1' bond. Thus, comparison with experiment is not possible. The agreement of calculated values with those measured from ENDOR spectra is clearly evident (signs, orders of values), especially when one keeps in mind that the experimental measurements were performed in the solid state on deoxyguanosine monophosphate while the calculations modeled an isolated deoxyribose molecule in vacuum. The agreement indicates that such calculations can be helpful in the interpretation and analysis of EPR or ENDOR spectra of carbon centered radicals.

Table 6. Enthalpies $\Delta H_{(298°)}$ for Hydrogen-Atom Abstraction from Different Positions of the Deoxyribose Ring

	$\Delta H_{(298°)}$ (kcal/mol)[a]			
	HF/6-31G	HF/6-31G*	MP2/6-31G*	MP-SAC2[b]
H_1	70.08	71.34	87.33	95.57
H_2	72.15	72.87	91.20	100.64
H_3	70.12	70.18	87.49	96.41
H_4	72.27	72.27	88.57	97.27

[a] $\Delta H_{(298°)}$ was calculated for the most stable conformers of deoxyribose and its radicals. [b] MP-SAC2 values refer to scaled MP2 calculations.[23]

Energetics of H-Atom Abstraction from Deoxyribose. An important factor that governs the formation of deoxyribose radicals is the energy needed to abstract a hydrogen from different sugar positions. The values obtained for abstraction of different hydrogens from deoxyribose, calculated at different theory levels, are displayed in Table 6.

The enthalpies of H-abstraction calculated at the HF level are highly underestimated judging by their increase with extending the basis set and inclusion of correlation. However, the order of the HF energies is the same as at the MP2/6-31G* calculations. Thus, calculations at the HF level can be used for some qualitative predictions. Scaling of the correlation energy (MP-SAC2), to account for the incomplete inclusion of correlation energy at the MP2 level, increases significantly the enthalpies for H-abstraction. This method of scaling of the correlation energy has been shown to be quite succesful in predictions of H-abstraction reaction energetics.[31] Experimental data for this reaction are not available, making it difficult to evaluate whether the MP-SAC2 energies could serve as reliable predictors of C–H bond energies in deoxyribose. However, the C–H bond strength in tetrahydrofuran, another model compound of deoxyribose, is only 92 kcal/mol.[32] Thus, it is possible, that the calculated MP2 energies are underestimated, while the MP-SAC2 energies are slightly overestimated. The correct enthalpies would probably lie somewhere between the values obtained with these two methods.

The observed order of H-abstraction enthalpies can be rationalized on the basis of C–H bond strengths of small model molecules. In CH_3OH and CH_3OCH_3, C–H bond strengths are the same, around 93 kcal/mol.[33] These bond strengths are 11 kcal/mol lower than those of CH_4.[33] This difference may explain why the C–H bonds to C_4, C_3, and C_1 have similar energies, which are significantly lower than that of the C_2–H bond. The former carbon atoms (C_4, C_3, and C_1) are directly attached to heteroatoms (oxygen or nitrogen) while the latter is not. Thus, abstraction from the C_2 carbon, which requires the highest energy, is expected to be the least likely.

The process of H-abstraction depends on two main factors: the barrier height, i.e. the activation energy, and the reactive

(31) Pardo, L.; Banfelder, J. R.; Osman, R. *J. Am. Chem. Soc.* **1992**, *114*, 2382–2390.
(32) Golden, D. M.; Benson, S. W. *Chem. Rev.* **1969**, *69*, 125.
(33) *CRC Handbook of Chemistry and Physics*; CRC Press, Inc.: Boca Raton, FL, 1984.

Table 7. Relative Rate Constants of H-Abstraction from Deoxyribose

	deoxyribose	nucleoside		A-DNA		B-DNA	
	k_{rel}[a]	A_{rel}[b]	$A_{rel}k_{rel}$[c]	A_{rel}[b]	$A_{rel}k_{rel}$[c]	A_{rel}[b]	$A_{rel}k_{rel}$[c]
H_1'	1.85	0.81	1.50	0.68	1.26	0.00	0.00
H_2'	0.26	1.97	0.51	0.25	0.06	0.24	0.06
H_3'	1.70	0.60	1.02	0.02	0.03	0.43	0.73
H_4'	1.00	1.00	1.00	1.00	1.00	1.00	1.00

[a] k_{rel} = relative rate constants in the isolated deoxyribose molecule estimated from the bond energies (see text). [b] A_{rel} = relative accessibilities of hydrogens in nucleosides and DNA.[32] [c] $A_{rel}k_{rel}$ = relative rate constants of H-abstraction in nucleosides and DNA.

cross section which is proportional to the accessible area of the abstracted hydrogen. In a previous work,[31] it was demonstrated that the barriers to H-abstraction correlate with C–H bond strengths. For example, the barriers for H-abstraction from methanol and from the C_α and C_β of ethanol, calculated at the MP2/6-31G* level, are 3.07, 0.61, and 4.35 kcal/mol, respectively. The corresponding C–H bond strengths calculated at the same level of theory are 85.66, 84.52, and 91.67 kcal/mol, and they clearly show the same rank order. The correlation between the bond strength and the barrier height suggests that a similar relation should exist between the bond strength and the rate constant. The relative rate constant based on the limited data available could be related to bond strength through the following expression:

$$k_{rel} = e^{-0.5\Delta\Delta H_{C-H}}$$

where the factor of 0.5 is derived empirically. On the basis of the data in Table 6, the rate constant for the H-abstraction of various hydrogens in deoxyribose relative to that of H_4 is shown in the first column of Table 7. Clearly, from energetic considerations, H_2 is the least probable hydrogen to be abstracted: its relative rate constant is approximately four times smaller than that of H_4. The rate constants for the abstraction of H_1 and H_3 are approximately 2-fold larger than for H_4. When the accessible surface areas of these hydrogens in a nucleoside are included, the relative constants become even more similar. The rate constant for H_2 is twice as small, and for H_1, it is bigger by 50% than H_4. The inclusion of the steric constraints imposed by the DNA structure has now a dramatic effect on the rate constants. In A-DNA, where the accessibility of H_2', and especially H_3', is considerably reduced, the relative rate constants of the abstraction of these hydrogens are reduced by a factor of 10–30 compared to those of H_4' and H_1'. In B-DNA, on the other hand, the accessibility of H_1' is virtually zero, leading to the situation where H_4' becomes the most accessible hydrogen for abstraction with H_3' a close competitor. These results illustrate the dependence of H-abstraction in DNA on two important elements. One is the strength of the scissile C–H bond that contributes to the chemical barrier for H-abstraction. The other is the accessibility to the abstracted hydrogen, which depends on the dynamic conformational properties of DNA. Even with such a simple model of accessibility, derived from a static description of DNA, the results presented in this work are in general agreement with the observation that the major product of H-abstraction in DNA is the C_4' radical.

Acknowledgment. This research was supported in part by the U.S. Department of Energy Grant DE-FG02-88ER60675. A generous grant of computer time from the University Computer Center of the City University of New York is gratefully acknowledged. We also thank the National Energy Reserach Supercomputer Center at Lawrence Livermore National Laboratory for providing computer time to perform the calculations in this work.